

# Short Papers

## Sensor-Based Exploration for Convex Bodies: A New Roadmap for a Convex-Shaped Robot

Ji Yeong Lee and Howie Choset

**Abstract**—We present a new roadmap that can be used to guide a convex body to explore an unknown planar workspace, i.e., to map an unknown configuration space diffeomorphic to  $SE(2)$ . This new roadmap is called the *convex hierarchical generalized Voronoi graph* (convex-HGVG). Since this roadmap is defined in terms of workspace distance information that is within line of sight of the convex body, we can use it to direct the robot to explore an unknown configuration space diffeomorphic to  $SE(2)$ . The challenge in defining the roadmap is that  $SE(2)$ , with holes removed from it, generally does not have a one-dimensional deformation retract. Therefore, we decompose the punctured  $SE(2)$  into contractible regions, in which we define convex generalized Voronoi graphs (convex-GVG), and then connect these graphs with additional structures called convex- $R$  edges. We formally show that the convex-HGVG, which is the union of the convex-GVG edges and the convex- $R$  edges, is indeed a roadmap.

**Index Terms**—Convex body, generalized Voronoi graph (GVG), motion planning, retract, roadmaps, sensor-based planning.

### I. INTRODUCTION

This paper presents a new sensor-based planning algorithm for a convex-shaped body to explore in an unknown planar workspace. In the past, most provably complete sensor-based planners [3], [13], [18] addressed many challenges, but were limited to robots modeled as point robots operating in the plane. To go beyond the planar environment, this paper develops an approach which is based on a structure called a *roadmap*. The roadmap, introduced by Canny [2], is a geometric structure that captures the connectivity of the free configuration space. A roadmap is a one-dimensional (1-D) network of curves with the following properties: accessibility, connectivity, and departability.

In this paper, we define a new roadmap termed the *convex hierarchical generalized Voronoi graph* (convex-HGVG). A planner can use this roadmap to determine a path for a convex body operating in an unknown 2-D workspace. A key feature of this roadmap is that it is defined in terms of the workspace distance function, i.e., the only information the planner requires is the workspace distance information, which can be easily provided by range sensors. This implies that using the convex-HGVG, the robot can explore unknown configuration spaces without explicitly constructing the configuration space.

The configuration space of the convex body operating in a plane is 3-D and diffeomorphic to  $SE(2)$ . The primary challenge in defining a roadmap for a convex body in  $SE(2)$  is that  $SE(2)$  with punctures (from configuration-space obstacles) is not contractible. This means that we cannot define a deformation retraction on the convex body's configuration space, as we could with the *generalized Voronoi diagram* (GVD) [16]. Instead, we decompose the free configuration space into contractible regions, called *junction regions*, define deformation retracts termed *convex-GVG edges* in each of the junction regions, and

then connect them using another structure called *R edges*, whose definition is based on the point-GVD of the workspace. Both of these edges are defined using a workspace-distance measurement. Therefore, the planner can construct a roadmap in the configuration space without explicitly constructing the configuration space. This implies that, unlike the methods which have to work in higher dimensional configuration spaces to construct a connected structure in the configuration space, the planner can infer the connectivity of the configuration space from the workspace connectivity using the convex-HGVG.

Since the convex-HGVG is a collection of edges and nodes, its definition naturally induces a sequence of reactive control laws, which are the low-level procedures by which a planner takes in sensory information and simultaneously builds up the map to direct the robot where to go for each type of edge, and arbitration schemes to select edges to explore at its nodes. This results in a reactive hybrid system that explores an unknown space. If the robot completes the construction of the convex-HGVG, then, in essence, it has explored the unknown space, because the planner can use the roadmap to plan future excursions into the space. It should be noted that a similar roadmap is also described in [19], which, however, does not prescribe an incremental construction method.

The outline of the paper is as follows. Section II reviews the prior work related to this paper. Section III formally defines the convex-HGVG, and Section IV shows that this roadmap has all desired properties; most importantly, the convex-HGVG forms a connected set in a connected configuration space. Finally, Section V summarizes the results and discusses future directions.

### II. PRIOR WORK

The convex-HGVG is one step toward the ultimate goal of sensor-based planning for highly articulated bodies, and one of the series of the roadmaps using the ideas based on the GVD for a point robot (see Fig. 1). The GVD is defined as the set of points equidistant to two obstacles (Fig. 2). Ó'Dúnlain and Yap [16] first applied the GVD to the robot-motion planning. They showed that the GVD is a deformation retract of a free space in a plane, and thus has the property of accessibility, connectivity, and departability. In other words, the GVD is a roadmap for the point robot in the plane. They applied GVD to path planning for a disk-shaped robot operating in the plane, however, their result required the full knowledge of the workspace.

Choset and Burdick [4] extended the GVD into three dimensions by defining the *generalized Voronoi graph* (GVG), which is the set of points equidistant to three obstacles. The GVG, by itself, is not connected in general, and thus additional structures, called higher order GVGs, were introduced, yielding a connected roadmap called the *hierarchical generalized Voronoi graph* (HGVG).

Early approaches [1], [7], [8], [15] which consider the rod or the polygonal/polyhedral bodies are, in general, restricted to the environments with the polygonal or polyhedral obstacles, and also require a full knowledge of the environment. These structures are defined in terms of the workspace-distance measurements, thus amenable to sensor-based implementations. The backbone of these structures is the set of configurations that are equidistant to  $n$  obstacles in an  $n$ -dimensional configuration space. The set of  $n$ -equidistant configurations results in a 1-D structure, but does not form a connected set, in general, except for the GVD in  $\mathbb{R}^2$ . Therefore, the challenge in these problems is to define new 1-D structures to connect those disconnected 1-D structures

Manuscript received May 1, 2003; revised February 9, 2004. This paper was recommended for publication by Associate Editor G. Oriolo and Editor I. Walker upon evaluation of the reviewers' comments.

The authors are with the Department of Mechanical Engineering, Carnegie Mellon University, Pittsburgh, PA 15213 USA (e-mail: jiyeeongl@andrew.cmu.edu; choset@cs.cmu.edu).

Digital Object Identifier 10.1109/TRO.2004.835454

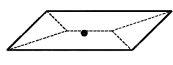
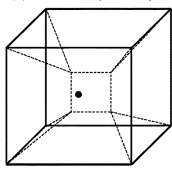
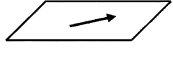
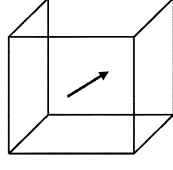
	Workspace : $\mathbb{R}^2$	Workspace : $\mathbb{R}^3$
Point	<p><b>GVD</b></p>  <p>Ó'Dúnlaing &amp; Yap [16] Choset &amp; Burdick [4]</p>	<p><b>HGVG:</b> <math>GVG(3) \cup GVG^2(2 \times 2)</math></p>  <p>Choset &amp; Burdick [4] Keerthi [8]</p>
Rod	<p><b>Rod-HGVG:</b> <math>Rod-GVG(3) \cup R-edge(2, \tan)</math></p>  <p>Ó'Dúnlaing &amp; Yap [15] Brooks [1] Choset &amp; Burdick [5]</p>	<p><b>Rod-HGVG:</b> Definitions &amp; Incremental Construction</p> 
Convex	<p><b>THIS PAPER</b></p> <p>Hoff et al. [10]</p>	<p>Manocha &amp; Lin [17] Hoff et al. [10]</p>
Highly Articulated Robot	<p>Long Term Goal</p>	

Fig. 1. Overview of roadmaps.

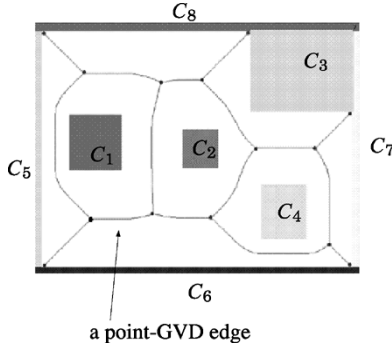


Fig. 2. Point-GVD or the GVD is the set of points equidistant to two obstacles.

to form a roadmap. Contrary to our method, most of the earlier works do not guarantee the connectivity of the roadmap, since they employ some heuristics to connect the disconnected components.

Recently, the probabilistic community has successfully demonstrated the capabilities of probabilistic roadmaps (PRM) for highly articulated robots [11], [12], [20]. One major benefit of the probabilistic approaches is that they do not construct the configuration space, but most of these approaches require knowledge of the work space prior to the planning event.

Yu *et al.* [21] developed a sensor-based PRM algorithm (called SBIC-PRM). This method incrementally expands the roadmap as the range sensor provides the newly visible workspace volume from the current robot configuration. Using this visible workspace-volume information, they can avoid the explicit computation of the configuration space, which is computationally expensive. However, the computation of the visible workspace volume itself could be expensive if the environment (or the current visible scene) or the geometry of the robot itself is complex. It is worth noting that, unlike our method, this method assumes a single range sensor installed at the end-effector of the robot.

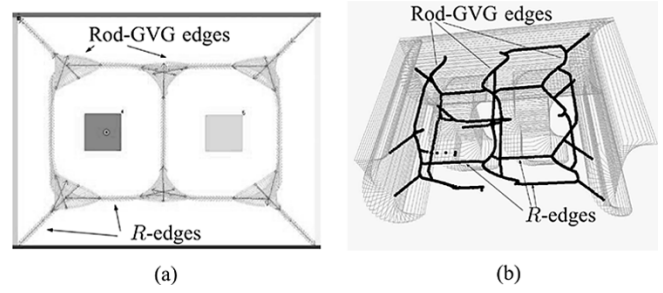


Fig. 3. Placements of the rod along a rod-HGVG in a rectangular enclosure with two rectangular obstacles in it. (a) Rod-HGVG. (b) Rod-HGVG in the configuration space.

It is also worth noting that Lin *et al.* [9], [10], [17] and others developed the algorithms that combine GVG with a probabilistic method to define a roadmap for the rigid bodies in 2-D and 3-D spaces. In [9], the planner aligns the “major axis” of the robot to the GVD to find a path, which is similar to our approach. However, their “alignment” does not necessarily produce a collision-free configuration, and the planner uses a probabilistic technique to find a collision-free path.

Choset *et al.* [5], [6] defined a roadmap, termed the *rod hierarchical generalized Voronoi graph* (rod-HGVG, Fig. 3), for rod-shaped robots operating in the plane. The rod-HGVG is also defined in terms of the workspace-distance function. Since the rod in a plane has three degrees of freedom (DOFs), a rod-GVG edge is defined to be the set of configurations equidistant to three obstacles. Unfortunately, the union of the rod-GVG edges is not necessarily connected, even in the planar case. To produce a connected structure, another type of edge is introduced, termed the *R edges*. Roughly speaking, the *R edges* are the two-way equidistant configurations which are tangent to point-GVD edges, thus, one can say they connect the disconnected rod-GVG edges using point-GVD edges. The rod-HGVG then comprises rod-GVG edges and *R edges*. The rod-HGVG forms a connected set in a connected configuration space (see [5] for a detailed proof). Essentially, we are forming an exact cellular decomposition of  $SE(2)$  where the rod-GVG edges are the deformation retract of the cells, and *R edges* connect the disconnected rod-GVG edges.

### III. CONVEX BODY OPERATING IN PLANE: DEFINITIONS

A convex body moving in the plane has three DOFs whose configuration space is diffeomorphic to  $SE(2)$ . Let  $q$  be the configuration of the convex body, then it can be represented as  $q = (x, y, \theta)^T$  (Fig. 4). Let  $R(q) \subset \mathbb{R}^2$  be the set of points that the convex body occupies in the plane when it is located at  $q$ . Also,  $P(q)$  and  $\theta(q)$  denote the position of the reference point<sup>1</sup> on the robot and the orientation of the robot, respectively. The distance between the obstacle  $C_i$  and the robot at  $q$  is defined as

$$D_i(q) = \min_{r \in R(q), c \in C_i} \|r - c\|. \quad (1)$$

See Fig. 4. This distance function can be measured using a series of range sensors along the boundary of the convex body. Then, to identify the obstacles using these sensors, one just needs to find the local minima of the sensor readings along the boundary of the convex body. That is, each local minima of the sensor reading corresponds to the distance to an obstacle. We denote the closest points on the robot (i.e., the point where one of the local minima is attained) at the configuration  $q$  to the obstacle  $C_i$  as  $r_i(q)$ , and the closest point on the obstacle  $C_i$  to the robot as  $c_i(q)$ , hence  $D_i(q) = \|r_i(q) - c_i(q)\|$ . We assume

<sup>1</sup>Note that the definition of convex-HGVG is independent of the choice of the reference point.

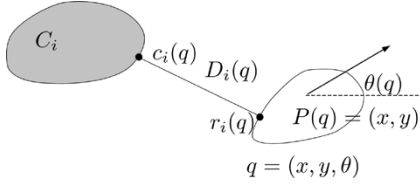


Fig. 4. Configuration of the convex body can be parameterized by  $(x, y, \theta)$ . Distance function between the obstacle  $C_i$  and the configuration  $q$  is defined as the minimum distance between the two point sets  $R(q)$  and  $C_i$ . The points  $r_i(q)$  and  $c_i(q)$  are the points closest on the robot and the obstacle  $C_i$  to each other.

that the robot is operating in a bounded 2-D workspace, populated by convex-shaped obstacles  $\{C_i\}$ . Nonconvex obstacles are modeled as the union of convex shapes. Note that the planner does not need to decompose explicitly a nonconvex obstacle into convex obstacles. (For an in-depth discussion of this, refer to [4].) Moreover, we assume that the points  $c_i(q)$  and  $r_i(q)$  are always uniquely defined. Note that if both the robot and an obstacle have flat edges, and the robot is oriented in such way that these two edges are parallel, then the points  $c_i(q)$  and  $r_i(q)$  cannot be uniquely defined. Essentially, we assume that the boundaries of the obstacles or the robot are “slightly curved” so that the points  $c_i(q)$  and  $r_i(q)$  are always uniquely identified.

#### A. Convex-GVG Edge

We use equidistance relationships to define the convex-HGVG. The first building block is the set of the configurations equidistant to two obstacles, termed *two-equidistant configuration face*, defined as

$$\text{CF}_{ij} = \{q \in SE(2) : 0 \leq D_i(q) = D_j(q) \leq D_h(q) \\ \forall h \neq i, j \text{ and } \nabla D_i(q) \neq \nabla D_j(q)\} \quad (2)$$

where  $\nabla D_i(q)$  is the gradient of the distance, which is derived in similar way as in [6]. The condition  $\nabla D_i(q) \neq \nabla D_j(q)$  is required to guarantee that the two-way equidistant configuration face is 2-D. Then the *convex generalized Voronoi diagram* (convex-GVD) is defined as union of  $\text{CF}_{ij}$ 's, i.e.,

$$\bigcup_i \bigcup_j \text{CF}_{ij}. \quad (3)$$

Convex-GVD forms a connected set, but is not a union of 1-D structures, since each  $\text{CF}_{ij}$  is a 2-D manifold. Now we define the convex-GVG edge as the set of configurations equidistant to three obstacles, which is formed by intersecting the above-defined two-way equidistant surfaces, which can be written as follows.

*Definition 1 (Convex-GVG Edge):*

$$\text{CF}_{ijk} = \text{CF}_{ij} \cap \text{CF}_{jk} \cap \text{CF}_{ik}. \quad (4)$$

Note that we cannot define  $\text{CF}_{ijk}$  as an intersection of just *two* two-way equidistant configuration faces, since we need to guarantee that the distance gradients to all three obstacles are distinct also. In other words, for the configuration  $q$  in the set  $\text{CF}_{ij} \cap \text{CF}_{ik}$ , it follows that  $D_i(q) = D_j(q) = D_k(q)$ , but it is not guaranteed that  $\nabla D_i(q) \neq \nabla D_k(q)$ , which is required to form a 1-D manifold.

If the convex body is small compared with the scale of the environment, a convex-GVG edge is diffeomorphic to  $S^1$ . Otherwise, a convex-GVG edge will have disconnected components, and its boundary elements are either *meet configurations* or *boundary configurations*. Meet configurations for the convex-GVG are the configurations equidistant to four obstacles, i.e.,

$$\text{CF}_{ijkl} = \text{CF}_{ijk} \cap \text{CF}_{ijl} \cap \text{CF}_{ikl} \cap \text{CF}_{jkl} \quad (5)$$

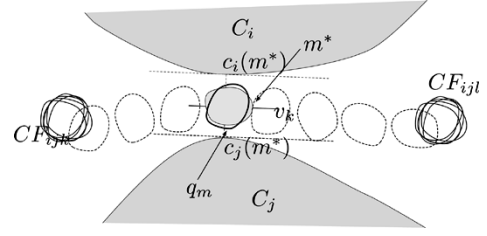


Fig. 5. Dotted robot positions represent a path between  $\text{CF}_{ijk}$  and  $\text{CF}_{ijl}$ . Along it, the minimum distance is attained at the configuration  $q_m$  (solid lines), and the distance at the  $q_m$  is larger than  $m^*$  (gray), which is oriented such that the principal squeeze axis is normal to  $c_i(m^*) - c_j(m^*)$ .

which is analogous to meet points for the point-GVG. Boundary configurations are the configurations where the distance to the closest obstacles becomes zero, i.e.,

$$B_{ijk} = \{q \in SE(2) : D_i(q) = D_j(q) = D_k(q) = 0\}. \quad (6)$$

*Definition 2 (Convex-GVG):* The **convex-GVG** is the union of convex-GVG edges, i.e., the set of configurations that are three-way equidistant which can be written as

$$\bigcup_{i=1}^{i=n-2} \bigcup_{j=i+1}^{j=n-1} \bigcup_{k=j+1}^{k=n} \text{CF}_{ijk}. \quad (7)$$

See Fig. 11 for an example of the swept volume of convex-GVG edges in a simple environment. Just like the rod-GVG, the convex-GVG is not necessarily connected, even in the planar case.

#### B. Convex-R Edges: Using Workspace Topology to Infer Configuration-Space Topology

We define a new structure, termed *convex-R edge*, to connect the disconnected components of the convex-GVG edges. Just like the *R* edges for the rod-GVG, we use the double equidistant configurations to connect disconnected convex-GVG edges. The set of two-way equidistant configurations forms a 2-D set, so we have to introduce another constraint. Roughly speaking, the double equidistance can be viewed as a constraint on position, and this additional constraint is on orientation. For the case of the rod, loosely speaking, there is a natural way to specify the orientation of the rod on the point-GVG edge, which is to make the rod “tangent” to the point-GVG edge. However, for a convex shape, there is no direct sense of tangency. The *R* edge definition for the convex body generalizes this notion of tangency for the convex body.

Consider two convex-GVG edges  $\text{CF}_{ijk}$  and  $\text{CF}_{ijl}$ , and assume that there is a path that passes between two obstacles  $C_i$  and  $C_j$  with end points  $q_k$  and  $q_l$  on  $\text{CF}_{ijk}$  and  $\text{CF}_{ijl}$ , respectively (Fig. 5). We can assume that this path is a two-way equidistant path, i.e., this path is a subset of the manifold  $\text{CF}_{ij}$ , since, given an arbitrary path, we can perform gradient ascent to each configuration in the path until it reaches a two-way equidistant configuration.

Each two-way equidistant path attains a local minimum of the distance along it. We want to consider only such paths for which this local minimum of  $D_i(q)$  is locally bigger than that of other two-way equidistant paths in a neighborhood. In other words, let  $\Pi_{ij}$  be the set of the two-way equidistant paths between  $\text{CF}_{ijk}$  and  $\text{CF}_{ijl}$  on  $\text{CF}_{ij}$ , i.e.,  $\Pi_{ij} = \{c \in C^0 | c(t) \in \text{CF}_{ij} \text{ for } t \in [0, 1] \text{ and } c(0) \in \text{CF}_{ijk} \text{ and } c(1) \in \text{CF}_{ijl}\}$ , where  $C^0$  denotes the set of continuous functions from  $[0, 1]$  to the free configuration space. Let  $\Gamma : \Pi_{ij} \rightarrow \mathbb{R}$  be a function such that  $\Gamma(c) = \min_{q \in c([0, 1])} D_i(q)$ . We consider only the paths which attain local maxima of  $\Gamma$  among the paths in  $\Pi_{ij}$ . Note that, in general, there can be infinitely many such paths, and our goal is to define *convex-R edge* as one of those paths.

To obtain such a path, we generalize the notion of tangency, using the concept of the *principal squeeze axes* (Fig. 6), defined as follows. Let

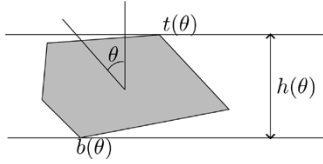


Fig. 6. Diameter function  $h(\theta)$ . The top (point  $t$ ) and bottom (point  $b$ ) determine the value of  $h(\theta)$ .

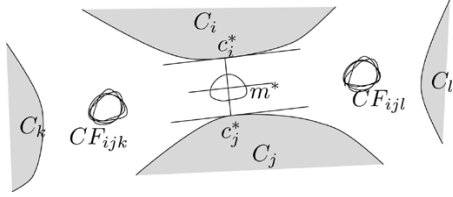


Fig. 7. Any path between  $CF_{ijk}$  and  $CF_{ijl}$  must “pass through” the line segment  $c_i^*c_j^*$ , where the distance between the two obstacles is determined. To maximize the minimum distance along the path, the robot must align its principal squeeze axis to the tangent of the obstacles at  $c_i^*$  (and  $c_j^*$ ). Note that convex- $R$  edge is defined such that it contains such a configuration.

$n$  be the unit vector in a reference direction and  $\theta$  be the orientation of the convex body with respect to  $n$ . Then, the value of diameter function [14]  $h : S^1 \rightarrow \mathbb{R}$  is defined to be  $\max_{t,b \in R(\theta)} (t - b) \cdot n$ , where  $R(\theta)$  is the set of the points occupied by a convex set  $R$  oriented at  $\theta$ . We call the two points  $t$  and  $b$  that determines the value of  $h(\theta)$  at given orientation as *top* and *bottom* points.

Note that for convex shapes, the diameter function has a finite number of local minima, and we use these minima to define the principal squeeze axes. Let  $t : S^1 \rightarrow \mathbb{R}^2$  and  $b : S^1 \rightarrow \mathbb{R}^2$  be the top and bottom points on a convex set in a body-fixed coordinate frame for a given orientation. Let  $\{\theta_i^*\}$  be the set orientations where the diameter function  $h$  obtains minimal values. A principal squeeze axis  $v_i$  is the unit vector that is normal to the vector  $(t(\theta_i^*) - b(\theta_i^*))$ . Note that there are always an even number of the principal squeeze axes for a given shape, since if the diameter function  $h(\theta)$  attains a local minimum at angle  $\theta_1$ , then  $h(\theta)$  attains a local minimum at  $\theta_1 + \pi$  also.

We now explain how the principal squeeze axes are used to define a path which locally maximizes the minimum distance along the path. This condition is as follows. Let  $c_i^*$  and  $c_j^*$  be the pair of closest points in  $C_i$  and  $C_j$ , i.e., the points in each obstacle where  $\|p_i - p_j\|$ ,  $p_i \in C_i$ ,  $p_j \in C_j$  is minimized, or  $(c_i^*, c_j^*) = \arg \min_{p_i \in C_i, p_j \in C_j} \|p_i - p_j\|$ . Then, the tangents of  $C_i$  and  $C_j$  at  $c_i^*$  and  $c_j^*$  must be parallel to each other, and also must be normal to the vector  $c_i^* - c_j^*$ . Clearly, if  $\|c_i^* - c_j^*\|$  is smaller than the diameter of the robot, there cannot be a (direct) path between  $CF_{ijk}$  and  $CF_{ijl}$ . Assuming otherwise, let us define a configuration  $m^*$  where the vector  $r_i(m^*) - r_j(m^*)$  in the plane is parallel to  $c_i^* - c_j^*$  and  $D_i(m^*) = D_j(m^*)$  (Fig. 7). Note that at this configuration  $m^*$ , the robot is located in between two parallel lines, both of which are tangent to the obstacles  $C_i$  and  $C_j$  at  $c_i^*$  and  $c_j^*$ , respectively. Also one of the principal squeeze axes,  $v_k$ , should be parallel to these parallel lines (see  $q_2$  in Fig. 8). Thus, for the path to attain the local maxima of the minimum distance, the vector  $c_i^* - c_j^*$  must be normal to a principal squeeze axis  $v_k$  when the robot is at the configuration where the distance to the obstacles has the smallest value on the path. Then it is clear that any path in  $\Pi_{ij}$  that does not contain  $m^*$  will have minimum distance bigger than  $D_i(m^*)$ . In other words, to attain the local maxima of the minimum distance, the path must contain  $m^*$ . In general, there will be infinitely many paths that contain  $m^*$ , and any one of those paths can be used to connect the two convex-GVG edges, and we define the convex- $R$  edge as one of those paths that can be constructed using sensor information.

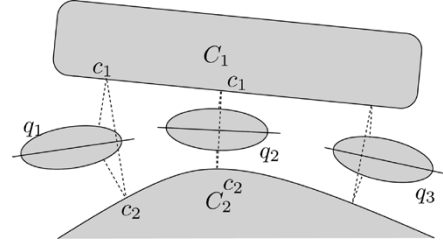


Fig. 8. Some placements of the robot in a convex- $R$  edge  $R_{12}$ . All the configuration shown in the figure are equidistant to  $C_1$  and  $C_2$ , and  $c_1 - c_2$  is normal to the principal squeeze axis of the robot.

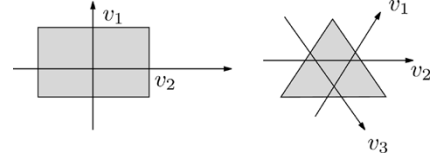


Fig. 9. Some examples of the principal squeeze axes for simple robots.  $v_i$ 's represent the principal squeeze axes. Note that we are only interested in the direction of the principal squeeze axis, not the “location” of the origin.

Now to obtain a specific path that passes through configuration  $m^*$ , we define the convex- $R$  edge as follows.

*Definition 3 (Convex- $R$  Edges):*

$$R_{ij} = \{q \in CF_{ij} \mid \langle c_i(q) - c_j(q), v_k \rangle = 0 \text{ for some } k\} \quad (8)$$

where the  $v_k$ 's are the principal squeeze axes of the robot (see Fig. 8 for some sample placements of the robot along a convex- $R$  edge).

The information required to define the convex- $R$  edges can readily be computed from the sensor information as follows. First, as we described above,  $r_i$  is the point where a local minimum of the sensor reading is attained along the boundary of the robot. Then since the vector  $c_i(q) - r_i(q)$  is normal to the tangent space of the robot at the point  $r_i(q)$ , and the length of  $c_i(q) - r_i(q)$  is the distance to the obstacle  $C_i$ , i.e., the value of the sensor reading at the point  $r_i$ , the location of  $c_i$  can easily be computed. Also,  $v_k$  is known, given the shape and the orientation of the robot. Therefore, the convex- $R$  edge is defined using only the information which can be computed from sensor data. As we noted above, there are always an even number of principal squeeze axes for a given convex body, and therefore, there are always an even number of convex- $R$  edges, given two obstacles  $C_i$  and  $C_j$ . Note that given a principal squeeze axis, there are two convex- $R$  edges associated with it, i.e., depending on how the principal squeeze axis aligns to the vector normal to  $c_i(q) - c_j(q)$ .

As noted before, for a general convex body, the diameter function can have multiple local minima (Fig. 9). Therefore, there would be more than two convex- $R$  edges that connect two adjacent convex-GVG edges, as shown in Fig. 10. In this example, the robot can rotate  $360^\circ$  on the left part of the environment, but cannot rotate fully on the right part. Thus, there are two convex-GVG edges,  $CF_{123}$ , which has one connected component, and  $CF_{234}$ , which has four components, disconnected from each other. The configurations  $q_1$  and  $q_2$  belong to the two different components of  $CF_{234}$ . Now for the robot to travel from  $q_1$  to  $q_2$ , it must move away from  $q_1$  to a “wide” region on the left, rotate, and then move back toward  $q_2$ . This explains why we need both of the convex- $R$  edges represented by dotted lines and dashed lines in Fig. 10, which correspond to each of the principal squeeze axes of the robot. The configurations  $m_1$  and  $m_2$  are the configurations along each component where the distance to the two closest obstacles is locally minimized, and the convex- $R$  edges are defined so that they contain these configurations  $m_1$  and  $m_2$ , respectively.

Then, the convex-HGVG is defined as follows.

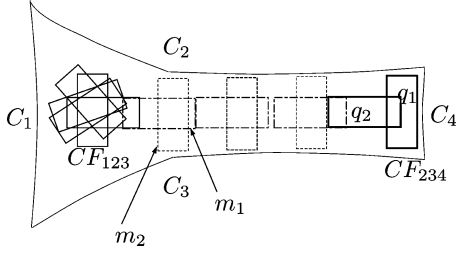


Fig. 10. In this environment, there are two convex-GVG edges,  $CF_{123}$  and  $CF_{234}$  (the configurations belonging to these convex-GVG edges are drawn in solid line), which are disconnected from each other. To form a connected roadmap, we need both of the convex- $R$  edges, represented by dotted lines and dashed lines, which correspond to each of the principal squeeze axes of the robot.

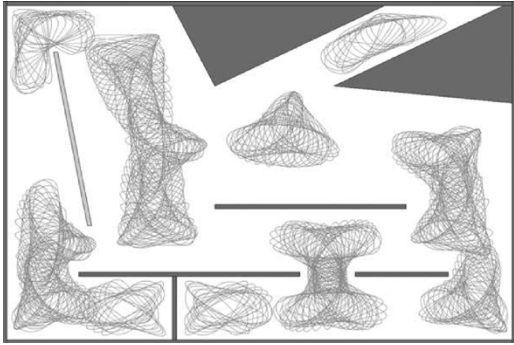


Fig. 11. Placements of the robot along the convex-GVG edges.

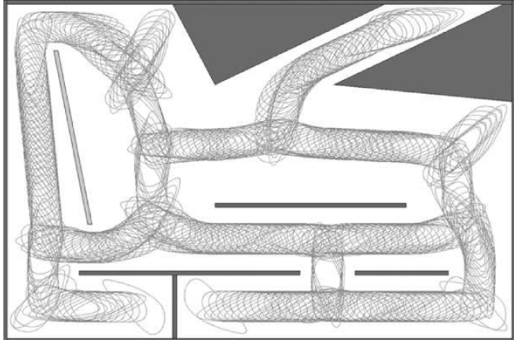


Fig. 12. Placements of the robot along convex- $R$  edges.

**Definition 4 (Convex-HGVG):** The convex-HGVG is the union of rod-GVG edges and convex- $R$  edges.

Figs. 11–13 show the swept volume of convex-HGVG for a robot with two principal squeeze axes. Therefore, two convex- $R$  edge components can be seen between two obstacles that define the convex- $R$  edge. Fig. 14 shows another example of the convex-HGVG, for a convex body with symmetries. In this example, the robot has the rectangular shape with a curved boundary, and is symmetric about two axes which are normal to each other. These symmetric axes are also principal squeeze axes. Therefore, there can be four convex- $R$  edges that connect two disconnected GVG edges. For example, note that in the lower left corner of the room, there are disconnected components of a GVG edge, and four convex- $R$  edges connect these disconnected components to the GVG edge on the lower right corner of the room.

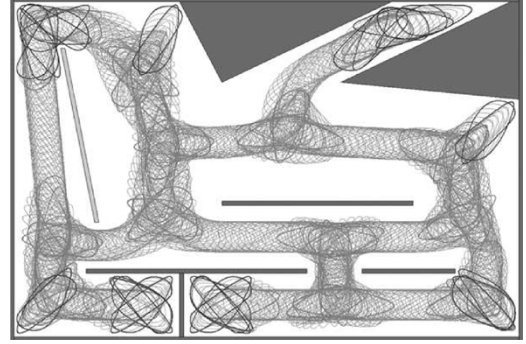


Fig. 13. Placements of the robot along the convex-HGVG.

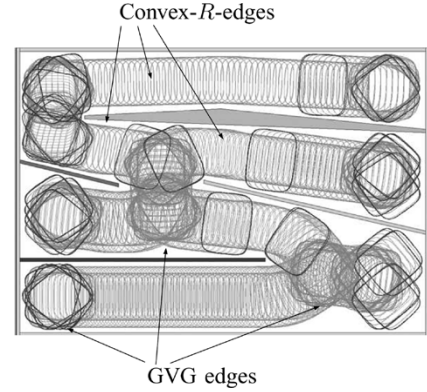


Fig. 14. Placements of the robot along the convex-HGVG.

### C. Control Laws and Incremental Construction Method

The convex-HGVG can be constructed incrementally using a root-tracing technique similar to that of the point-based GVG [3]. For generating a convex-GVG edge, the planner traces the roots of the expression

$$G(q) = \begin{bmatrix} D_i(q) - D_j(q) \\ D_i(q) - D_k(q) \end{bmatrix} \quad (9)$$

and for the convex- $R$  edges, the planner traces the roots of the

$$G(q) = \begin{bmatrix} D_i(q) - D_j(q) \\ \langle v_s, (c_i - c_j) \rangle \end{bmatrix} \quad (10)$$

according to the control law

$$\dot{q} = \alpha V (\nabla G(q)) + \beta (\nabla G(q))^\dagger G(q) \quad (11)$$

where:

- $\alpha$  and  $\beta$  are scalar gains;
- $\nabla G$  is the gradient of  $G$ ;
- $V \in \text{Null}(\nabla G(q))$ , the null space of  $\nabla G(q)$ ;
- $(\nabla G(q))^\dagger$  is the Penrose pseudoinverse of  $\nabla G(q)$ , i.e.,

$$(\nabla G(q))^\dagger = (\nabla G(q))^T \left( \nabla G(q) (\nabla G(q))^T \right)^{-1}. \quad (12)$$

## IV. ROADMAP PROPERTIES

### A. Accessibility

Accessibility is the property that the robot can move onto a configuration in the roadmap from an arbitrary configuration. We show that the robot can reach a configuration on a convex-GVG edge using a sequence of fixed-orientation gradient ascents of the distance function to

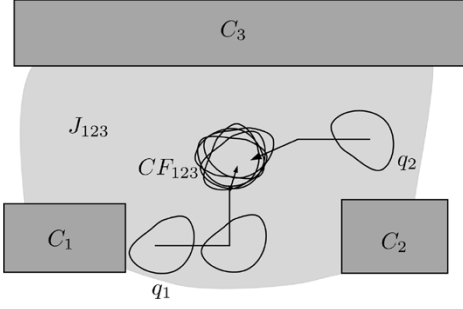


Fig. 15. Accessibility is accomplished by a successive application of fixed-orientation gradient ascent. The access path is represented by arrows. Note that  $\theta(q_i) = H(\theta(q_i), 1)$ . If  $q_1, q_2$  both belong to the same junction region  $J_{123}$ , then, by definition, they both access a connected component of  $CF_{123}$ . This means that there exists a path between  $q_1$  and  $q_2$  which lies entirely in  $J_{123}$ .

the closest obstacles. Let  $C_i$  be the closest obstacle to the convex body at a given configuration  $q$ . Then, while maintaining a fixed orientation, the robot moves away from  $C_i$  until it is double equidistant with an obstacle  $C_j$ , i.e., it follows the path defined by the differential equation

$$\dot{c}_1(t) = \tilde{\nabla} D_i(c_1(t)) \quad (13)$$

where  $\tilde{\nabla} D_i$  is the distance gradient projected onto the  $xy$  plane. Then the robot moves away from  $C_i$  and  $C_j$  while maintaining double equidistance, until it becomes three-way equidistant, i.e., it follows the path defined by

$$\dot{c}_2(t) = \pi_{T_{c_2(t)} CF_{ij}} \tilde{\nabla} D_i(c_2(t)) \quad (14)$$

where  $\pi$  is the projection operator. Then, as in the case of the rod, we have the following results, whose proofs are identical to the case of the planar rod [6].

**Theorem 1 (Accessibility):** In a bounded environment, the convex-GVG has the accessibility property for all configurations in the free configuration space.

The functions  $c_1$  and  $c_2$  implicitly define the accessibility function  $H(q, t)$ . In other words,  $H$  is a mapping from  $FS \times [0, 1]$  to  $\cup CF_{ijk}$  that satisfies  $H(q, 0) = q$ ,  $H(q, 1) \in \cup CF_{ijk}$ , and  $\theta(H(q, t)) = \theta(q)$  for all  $t \in [0, 1]$ . We assume that the parameter  $t$  is scaled appropriately. In general,  $H$  is not a continuous function, which can be seen easily from the fact that there are multiple convex-GVG edges disconnected from each other in a connected configuration space. To “make  $H$  continuous,” we define the *junction region*  $J_{ijk}$ , in the planar rod-HGVG, as a pre-image of a convex-GVG edge  $CF_{ijk}$  under the accessibility function  $H$ , i.e., the junction region  $J_{ijk}$  is the set of configurations that access the convex-GVG edge  $CF_{ijk}$  (Fig. 15), which can be written as follows.

**Definition 5 (Junction Regions):**

$$J_{ijk} = \{q \in SE(2) : H(q, 1) \in CF_{ijk}\}. \quad (15)$$

Then it can be shown that  $H$  is continuous in a connected component of a junction region  $J_{ijk}$ , and therefore,  $CF_{ijk}$  can be viewed as the deformation retract of  $J_{ijk}$  under  $H$ . The proof of this is identical to the case of the planar rod, which can be found in [6]. Note that the union of the junction regions is the free configuration space (Fig. 16), which follows from *Theorem 1*. Two junction regions are said to be *adjacent* if they share a boundary, and we assume that the configuration on the shared boundary can access either convex-GVG edge. This implies that, if two junction regions are adjacent, there is a path (which does not necessarily lie on convex-HGVG) between the convex-GVG edges associated with those junction regions.

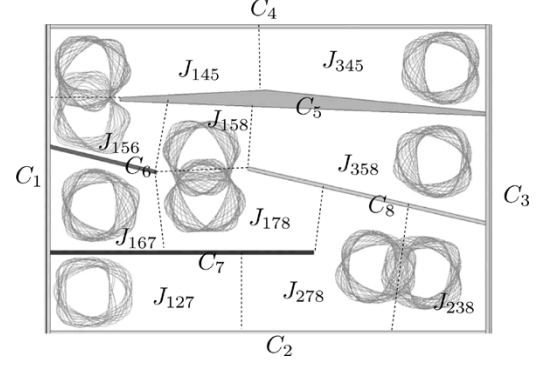


Fig. 16. Free configuration space is decomposed into junction regions. This figure actually shows the “swept volume” of the junction regions.

### B. Connectivity and Construction of the Convex- $R$ Edge

In this section, we prove the connectivity of the convex-HGVG, which can be stated formally as follows.

**Theorem 2 (Connectivity):** Let  $q_s$  and  $q_g$  be two configurations in free configuration space, and  $H(q_s, 1)$  and  $H(q_g, 1)$  be the accessed configuration on convex-HGVG for  $q_s$  and  $q_g$ , respectively. Then, there is a path between  $q_s$  and  $q_g$ , if and only if there exists a path between  $H(q_s, 1)$  and  $H(q_g, 1)$  that lies entirely on convex-HGVG.

Note that if  $q_s$  and  $q_g$  belong to the same connected component of junction region, then trivially, there is a path between  $H(q_s, 1)$  and  $H(q_g, 1)$  on convex-HGVG, since  $H(q_s, 1)$  and  $H(q_g, 1)$  both belong to the same connected component of a convex-HGVG edge. Therefore, the central part of the proof is to show that convex- $R$  edges connect two convex-GVG edges associated with two adjacent junction regions. Our strategy is to show that given a principal squeeze axis  $v_k$ , the configuration that satisfies the convex- $R$  edge condition varies continuously as the distance to the closest obstacle changes. Then we can “construct” a path away from the configuration  $m^*$  as the distance increases, until the configuration becomes three-way equidistant. First, we show that given  $\delta \in \mathbb{R}$ , which is larger than the value  $D(m^*)$  and a principal squeeze axis  $v_k$ , we can find the configurations that satisfy the convex- $R$  edge condition. Note that there will be four such configurations, because the robot can move in both directions away from  $m^*$  in two different orientations.

**Lemma 1:** Given a principal squeeze axis  $v_k$ , a distance  $\delta > D(m^*)$ , there are four configurations that satisfy the convex- $R$  edge condition, i.e., there are four configurations  $q$  such that  $D_i(q) = D_j(q) = \delta$  and  $\langle c_i(q) - c_j(q), v_k \rangle = 0$ .

**Proof:** Recall that there are two convex- $R$  edges associated with  $C_i$  and  $C_j$  for a given principal squeeze axis  $v_k$ , and as the robot travels along the convex- $R$  edges, there will be two configurations on each of these two convex- $R$  edges that satisfy  $D_i(q) = D_j(q) = \delta$ . In the following proof, we show that there is one configuration on one “side” of the *one* convex- $R$  edge that satisfies the conditions specified in the statement of the lemma. We show this by contradiction. Now given a configuration  $q$  on an convex- $R$  edge with  $D_i(q) = D_j(q) = \delta$ , consider a robot whose outer boundary is expanded by  $\delta$ , so that  $r_i(q) = c_i(q)$  and  $r_j(q) = c_j(q)$  for this expanded robot.<sup>2</sup> Note that for the extended shape,  $c_i$  and  $c_j$  do not change, and the  $v_k$  is still a principal squeeze axis. Let  $b_k$  and  $t_k$  be the top and bottom points associated with the given principal squeeze axis  $v_k$ , and let  $c_i^*$  and  $c_j^*$  be the closest points on  $C_i$  and  $C_j$ . Also let  $\phi_i(q)$  be the angle between

<sup>2</sup>To be precise, we need to define a new configuration space and a new symbol for the configuration of the expanded robot, but this will make the proof unnecessarily complex.

the vector  $c_i(q) - c_j(q)$  and the tangent of the robot boundary at point  $c_i(q)$ .

Now, assume that there are two configurations  $q_1$  and  $q_2$  on  $CF_{ij}$  such that  $D_i(q_1) = D_i(q_2) = \delta$ ,  $\langle c_i(q_1) - c_j(q_1), v_k \rangle = 0$ , and  $\langle c_i(q_2) - c_j(q_2), v_k \rangle = 0$ . This implies that  $c_i(q_1) - c_j(q_1)$  and  $c_i(q_2) - c_j(q_2)$  are both parallel to the vector  $t_k - b_k$ . Since the robot is convex,  $\|c_i(q_1) - c_j(q_1)\| \neq \|c_i(q_2) - c_j(q_2)\|$  if  $q_1 \neq q_2$ . Assume, without loss of generality,  $\|c_i(q_1) - c_j(q_1)\| > \|c_i(q_2) - c_j(q_2)\|$ . This implies that the vector  $c_i(q_1) - c_j(q_1)$  is closer to the vector  $t_k - b_k$  than  $c_i(q_2) - c_j(q_2)$ , and in turn, this implies that  $\phi_i(q_1) > \phi_i(q_2)$  and  $\phi_j(q_1) > \phi_j(q_2)$ .

Now we consider the locations of  $c_i$  and  $c_j$  on the boundary of the obstacles. Note that at  $c_i$ , the tangents of the robot boundary and the obstacle boundary coincide. Therefore,  $\phi_i(q)$  is also the angle between the vector  $c_i(q) - c_j(q)$  and the tangent of the obstacle boundary at point  $c_i(q)$ . There are three possibilities: 1)  $c_i(q_1) = c_i(q_2)$ ; 2)  $c_i(q_2)$  gets closer to  $c_i^*$  than  $c_i(q_1)$ ; and 3)  $c_i(q_2)$  gets farther from  $c_i^*$  than  $c_i(q_1)$ . For cases 1) and 3), from the assumption,  $c_j(q_2)$  must be closer to  $c_j^*$  than  $c_j(q_1)$ . Otherwise, from the convexity of the obstacles,  $\|c_i(q_1) - c_j(q_1)\| < \|c_i(q_2) - c_j(q_2)\|$ . This results in  $\phi_j(q_2) > \phi_j(q_1)$ , which is a contradiction. For case 2), again from the convexity of the obstacles,  $\phi_i(q_2) + \phi_j(q_2) > \phi_i(q_1) + \phi_j(q_1)$ , which is also a contradiction. Therefore, there can be only one configuration that satisfies the convex- $R$  edge condition, given  $\delta$  on one "side" of the convex- $R$  edge. ■

*Lemma 2:* Let  $q_1$  be a configuration in  $CF_{ijk}$  and  $q_2$  be a configuration in  $CF_{ijl}$ . If there exists a path  $s$  between  $q_1$  and  $q_2$ , then there exists an convex- $R$  edge  $R_{ij}$  that connects  $CF_{ijk}$  and  $CF_{ijl}$ , i.e., the union of  $CF_{ijk}$ ,  $CF_{ijl}$ , and  $R_{ij}$  is a connected set. In other words, there is a path between  $H(q_1, 1)$  and  $H(q_2, 1)$  which lies completely on convex-HGVG.

*Proof:* From the observation above, there is a saddle point  $m^*$  of the distance on  $CF_{ij}$  if there is a path between  $CF_{ijk}$  and  $CF_{ijl}$ , and  $m^*$  is in  $R_{ij}$ . We now show that we can grow the convex- $R$  edge from  $m^*$  in both directions as we increase the distance from the obstacles. First, take a small neighborhood  $B(m^*)$ , then since  $R_{ij}$  is a 1-D manifold, it contains some configurations in  $R_{ij}$ , and since the  $m^*$  is a saddle point, and there is only one unique configuration with distance  $D_i(m^*)$  on  $R_{ij}$  (*Lemma 1*), there must be a configuration  $q_1$  in  $B(m^*)$  with  $D_i(q_1) > D_i(m^*)$ . Now consider a neighborhood  $B(q_1)$  of  $q_1$ . Using a similar argument, it contains a configuration  $q_2$  such that  $D_i(q_2) > D_i(q_1)$ . Therefore, the distance to the closest obstacles monotonically increases as the robot moves away from the saddle point  $m^*$ , and since the environment is bounded, the convex- $R$  edge  $R_{ij}$  terminates at a three-way equidistant configuration. ■

Finally, we prove *Theorem 2*.

*Proof:* If there is a path between  $H(q_s, 1)$  and  $H(q_g, 1)$  which lies entirely on convex-HGVG, then it is obvious that there exists a path between  $q_s$  and  $q_g$ , since there exist paths between  $q_s$  and  $H(q_s, 1)$  and between  $q_g$  and  $H(q_g, 1)$ , from accessibility.

Now, assume there exists a path  $c(t)$  between  $q_s$  and  $q_g$ , i.e.,  $c \in C^0$ ,  $c(0) = q_s$ ,  $c(1) = q_g$ , and  $c(t)$  are in free configuration space for all  $t \in [0, 1]$ . As noted above, if  $q_s$  and  $q_g$  belong to a same connected component of a junction region, it is trivial.

Now assume that  $q_s$  and  $q_g$  belongs to two different junction regions. Let us denote  $q_s$  as  $q_0$  and  $q_g$  as  $q_{n+1}$ , and let  $J_0$  and  $J_{n+1}$  be the junction regions that contain  $q_0$  and  $q_{n+1}$ , respectively. Also, let  $J_0, J_1, J_2, \dots, J_n, J_{n+1}$  be the sequence of the junction regions that the path  $c(t)$  passes through. Then  $J_i$  and  $J_{i+1}$  (for  $i = 0$  to  $n$ ) are adjacent to each other. Let  $q_i$  be a configuration on  $c(t)$  which is contained in the junction region  $J_i$ , and let  $H(q_i, 1)$  be the accessed configuration on convex-HGVG for  $q_i$ . Then, since  $J_i$  and  $J_{i+1}$  are adjacent to each other, from *Lemma 2*, there exists a path between  $H(q_i, 1)$

and  $H(q_{i+1}, 1)$  which lies on convex-HGVG. This implies there exists a path between  $H(q_s, 1)$  and  $H(q_g, 1)$  on convex-HGVG, which is a concatenation of the paths between  $H(q_i, 1)$  and  $H(q_{i+1}, 1)$  for  $i = 0$  to  $n$ . ■

## V. CONCLUSION

This paper introduces a new roadmap called the convex-HGVG for a convex body operating in a 2-D workspace. The convex-HGVG is defined in terms of workspace-distance information, which is within line of sight of the robot and thus can be implemented in a sensor-based manner. The convex-HGVG comprises two components: 1) convex-GVG edges, which are three-way equidistant; and 2) convex- $R$  edges, which are two-way equidistant paths that connect disconnected convex-GVG edges. The use of  $R$  edges was inspired by the rod-HGVG, where the rod is tangent to a point-GVG structure. However, in this paper, using the principal squeeze axis, we generalized the definition of tangency for convex bodies.

We chose this definition because  $SE(2)$ , with arbitrary holes removed from it, does not have a 1-D deformation retract. Instead, we break down  $SE(2)$  into contractible regions, each having its own convex-GVG, and connect the regions with convex- $R$  edges. What is interesting here is that convex- $R$  edges are essentially a topological representation of the workspace, but we are using them to infer topological properties of the configuration space.

Since this roadmap is defined in terms of workspace-distance information, we can prescribe a sensor-based incremental method to construct the convex-HGVG edges without constructing the configuration space, which is important for sensor-based planning, since the configuration space cannot be constructed without the prior knowledge about the workspace. Furthermore, the convex-HGVG can be seen as a collection of edges and nodes, where the edges are either convex-GVG edges or convex- $R$  edges, and the nodes are the meet configurations (i.e., intersection of two convex-GVG edges) or the configuration where a convex-GVG edge and a convex- $R$  edge intersect. Therefore, the incremental construction method induces a reactive control law for the robot to explore an unknown configuration space, i.e., the robot can invoke the appropriate control law (edge-tracing procedure) for each type of edge, and choose which edges to explore on each node.

As we mentioned before, this paper is a step toward the ultimate goal of sensor-based planning for an articulated multibody robot, which can be modeled as multiple rods or convex bodies connected together. The next step in this chain of research is to extend the current result to a convex body operating in a 3-D workspace and a two-convex body operating in a 2-D and 3-D workspace.

## REFERENCES

- [1] R. A. Brooks, "Solving the find-path problem by good representation of free space," *IEEE Trans. Syst., Man, Cybern.*, vol. SMC-13, no. 3, pp. 190–197, Mar.-Apr. 1983.
- [2] J. F. Canny, *The Complexity of Robot Motion Planning*. Cambridge, MA: MIT Press, 1988.
- [3] H. Choset and J. Burdick, "Sensor-based motion planning: Incremental construction of the hierarchical generalized Voronoi graph," *Int. J. Robot. Res.*, vol. 19, no. 2, pp. 126–148, Feb. 2000.
- [4] —, "Sensor-based motion planning: The hierarchical generalized Voronoi graph," *Int. J. Robot. Res.*, vol. 19, no. 2, pp. 96–125, Feb. 2000.
- [5] H. Choset and J. W. Burdick, "Sensor-based planning for a planar rod robot," in *Proc. IEEE Int. Conf. Robot. Autom.*, 1996, pp. 3584–3591.
- [6] H. Choset and J. Y. Lee, "Sensor-based construction of a retract-like structure for a planar rod robot," *IEEE Trans. Robot. Autom.*, vol. 17, no. 4, pp. 435–449, Aug. 2001.
- [7] J. Cox and C. K. Yap, "On-line motion planning: Case of a planar rod," *Ann. Math. Artif. Intell.*, vol. 3, pp. 1–20, 1991.

- [8] A. Dattasharma and S. S. Keerthi, "An augmented Voronoi roadmap for 3D translational motion planning for a convex polyhedron moving amidst convex polyhedral obstacles," *Theoretical Computer Sci.*, vol. 140, no. 2, pp. 205–230, Apr. 1995.
- [9] M. Frosky, M. Garber, M. Lin, and D. Manocha, "A Voronoi-based hybrid motion planner," in *Proc. IEEE Int. Conf. Intell. Robots Syst.*, 2001, pp. 55–60.
- [10] K. Hoff, T. Culver, J. Key, M. Lin, and D. Manocha, "Interactive motion planning using hardware-accelerated computation of generalized Voronoi diagrams," in *Proc. IEEE Int. Conf. Robot. Autom.*, 2000, pp. 1931–1937.
- [11] L. Kavraki, P. Svestka, J.-C. Latombe, and M. Overmars, "Probabilistic roadmaps for path planning in high-dimensional configuration spaces," *IEEE Trans. Robot. Autom.*, vol. 12, no. 4, pp. 566–580, Aug. 1996.
- [12] J. J. Kuffner and S. M. LaValle, "RRT-connect: An efficient approach to single-query path planning," in *Proc. IEEE Int. Conf. Robot. Autom.*, 2000, pp. 995–1001.
- [13] V. Lumelsky and A. Stepanov, "Path planning strategies for point mobile automaton moving amidst unknown obstacles of arbitrary shape," *Algorithmica*, vol. 2, pp. 403–430, 1987.
- [14] M. Mason, K. Y. Goldberg, and R. H. Taylor, "Planning sequences of squeeze-grasps to orient and grasp polygonal objects," in *Proc. 7th CISM-IFTOMM Symp. Theory, Practice Robots, Manipulators*, 1988, pp. 531–538.
- [15] C. Ó'Dúnlaing, M. Sharir, and C. K. Yap, "Generalized Voronoi diagrams for moving a ladder. I: Topological analysis," *Commun. Pure Appl. Math.*, vol. 39, pp. 423–483, 1986.
- [16] C. Ó'Dúnlaing and C. K. Yap, "A "retraction" method for planning the motion of a disc," *J. Algorithms*, vol. 6, pp. 104–111, 1985.
- [17] C. Pisula, K. Hoff, M. Lin, and D. Manocha, "Randomized path planning for a rigid body based on hardware accelerated Voronoi sampling," in *Proc. Workshop Algorithmic Foundations Robot.*, 2000, pp. 279–292.
- [18] N. S. V. Rao, S. Karetí, W. Shi, and S. S. Iyenagar, "Robot navigation in unknown terrains: Introductory survey of non-heuristic algorithms," Oak Ridge Nat. Lab., Oak Ridge, TN, Rep. ORNL/TM-12410:1-58, Jul. 1993.
- [19] S. Rusaw, "Sensor-based motion planning in  $SE(2)$  and  $SE(3)$  via nonsmooth analysis," Univ. Oxford, Oxford, U.K., Tech. Rep. PRG-RR-01-13, Aug. 2001.
- [20] S. A. Wilmarth, N. M. Amato, and P. F. Stiller, "Motion planning for a rigid body using random networks on the medial axis of the free space," in *Proc. 15th Annu. ACM Symp. Computat. Geom.*, Jun. 1999, pp. 173–180.
- [21] Y. Yu and K. Gupta, "Sensor-based probabilistic roadmaps: experiments with an eye-in-hand system," *Adv. Robot.*, vol. 41, no. 6, pp. 515–536, 2000.

## Robot Steering With Spectral Image Information

Christopher Ackerman and Laurent Itti

**Abstract**—We introduce a method for rapidly classifying visual scenes globally along a small number of navigationally relevant dimensions: depth of scene, presence of obstacles, path versus nonpath, and orientation of path. We show that the algorithm reliably classifies scenes in terms of these high-level features, based on global or coarsely localized spectral analysis analogous to early-stage biological vision. We use this analysis to implement a real-time visual navigation system on a mobile robot, trained online by a human operator. We demonstrate successful training and subsequent autonomous path following for two different outdoor environments, a running track and a concrete trail. Our success with this technique suggests a general applicability to autonomous robot navigation in a variety of environments.

**Index Terms**—Autonomous robot, Fourier transform, gist of a scene, navigation, path following, vision.

### I. INTRODUCTION

Previous use of vision for robot navigation has often assumed a known or otherwise highly constrained environment [1]. In particular, successful autonomous indoor and outdoor navigation has been demonstrated with model-based approaches, where a robot compares a manually specified or learned geometric model of the world to its sensory inputs [2]. However, these approaches are limited by design to environments amenable to geometric modeling, and where reliable landmark points are available for model matching [3], [4].

Model-free or mapless algorithms have been proposed to address these limitations. In "view-based" mapless approaches, scene snapshots and associated motor commands are memorized along a route during training. During autonomous navigation, incoming images are matched against learned ones, to look up motor commands [5]. Images of the training environment may be stored explicitly and matched against new inputs by cross-correlation [6]. Effective in small environments, such approaches tend to generalize poorly (new scenes must correlate with learned ones), and require prohibitive memory and computation in larger environments. To alleviate these requirements, learned information may be implicitly stored in the weights of a trained neural network; typically, then, images are first reduced to a few landmark or characteristic regions, to reduce network complexity [7], [8]. Finally, computationally expensive algorithms involving much image processing and segmentation [9], including texture recognition [10], [11], stereo vision [12], or large rule sets [13] have been proposed to understand the environment. Although less explicit than model-based approaches, these algorithms also tend to incorporate a high degree of world knowledge and assumed environmental structure through design and tuning of feature detectors and rule bases. Here we take inspiration from biological vision in developing a mapless system with low memory, computation, and world-knowledge requirements.

The early stages of visual processing in the primate (including human) brain are believed, in a first approximation, to be organized in

---

Manuscript received March 22, 2004. This paper was recommended for publication by Associate Editor J. Kosecka and Editor S. Hutchinson upon evaluation of the reviewers' comments. This work was supported in part by the National Science Foundation, in part by the National Eye Institute, in part by the National Geospatial Intelligence Agency, and in part by the Zumberge Research Innovation Faculty Fund.

The authors are with the Computer Science Department, University of Southern California, Los Angeles, CA 90089 USA (e-mail: christopher.ackerman@gmail.com; itti@pollux.usc.edu).

Digital Object Identifier 10.1109/TRO.2004.837241